PHOTONICS Research

Auxiliary-cavity-assisted vacuum Rabi splitting of a semiconductor quantum dot in a photonic crystal nanocavity

Hua-Jun Chen

School of Mechanics and Photoelectric Physics, Anhui University of Science and Technology, Huainan 232001, China (chenphysics@126.com)

Received 14 September 2018; revised 8 October 2018; accepted 27 October 2018; posted 31 October 2018 (Doc. ID 345940); published 30 November 2018

The coherent light-matter interaction has drawn an enormous amount of attention for its fundamental importance in the cavity quantum-electrodynamics (C-QED) field and great potential in quantum information applications. Here, we design a hybrid C-QED system consisting of a quantum dot (QD) driven by two-tone fields implanted in a photonic crystal (PhC) cavity coupled to an auxiliary cavity with a single-mode waveguide and investigate the hybrid system operating in the weak, intermediate, and strong coupling regimes of the light-matter interaction via comparing the QD-photon interaction with the dipole decay rate and the cavity field decay rate. The results indicate that the auxiliary cavity plays a key role in the hybrid system, which affords a quantum channel to influence the absorption of the probe field. By controlling the coupling strength between the auxiliary cavity and the PhC cavity, the phenomenon of the Mollow triplet can appear in the intermediate coupling regime, and even in the weak coupling regime. We further study the strong coupling interaction manifested by vacuum Rabi splitting in the absorption with manipulating the cavity-cavity coupling under different parameter regimes. This study provides a promising platform for understanding the dynamics of QD-C-QED systems and paving the way toward on-chip QD-based nanophotonic devices.

https://doi.org/10.1364/PRJ.6.001171

1. INTRODUCTION

Cavity quantum electrodynamics (C-QED) [1,2], researching the physics of an interaction system including a single quantum emitter and a single radiation mode and classifying the interactions into weak, intermediate, and strong coupling regimes, has drawn tremendous attention not only because it provides a test bed for quantum physics, but also because it has potential applications in quantum information processing [3–7]. Semiconductor nanostructures coupled to optical resonators, such as a single quantum dot (QD)–semiconductor microcavity system [8], a single QD embedded in a microdisk microcavity system [9], and photonic crystal (PhC) micro/nanocavities with self-assembled QD systems [10], are a fascinating platform for studying solid-state C-QED systems. In particular, PhC nanocavities coupled to QDs are some of the most advanced systems for studying C-QED and constructing devices for quantum information processing due to their strong light-matter interactions originating from the tight optical confinement of the nanocavities. Based on the QD-microcavity systems, various remarkable quantum phenomena have been revealed, including laser oscillation [11], spontaneous emission control [12], single-photon sources [13], quantum entanglement [14], and vacuum Rabi splitting (VRS) [8,10,15].

For coherent manipulation, a key prerequisite is to reach the strong coupling regime, where the emitter-photon coupling strength becomes larger than the decay rates of the emitter and the cavity field decay rate. Strong light-matter coupling manifested by VRS has been observed in QD-C-QED systems [8,10], which have been employed for developing various classical and quantum optical devices, such as optical switches [16,17], nonclassical light generators [18], and quantum gates [19]. Since the first observation of the VRS in a solid-state system composed of QDs and PhC cavities [10], this system has been considered as a great candidate for realizing strong coupling between QDs and a microcavity. In the past decades, great efforts have been made in the investigation of C-QED focusing on a single quantum emitter inside a cavity [11,15,20–22], and how to improve the quality factor and reduce the mode volume of the resonators for realizing stronger interactions. Recently, Liu *et al.* [23] have presented a protocol for realizing effective strong coupling in a highly dissipative C-QED system, where a highly dissipative cavity interacted simultaneously with a single emitter and an auxiliary cavity with a high quality factor but a large volume. Their results have shown that the vacuum Rabi oscillation occurs for a single

quantum emitter inside a cavity even with the bosonic decay-to-interaction rate ratio exceeding 10^2, when the photon field is coupled to an auxiliary high-Q cavity.

In this paper, we consider a hybrid QD-PhC nanocavity system, where the QD driven by two-tone fields is embedded in a PhC nanocavity coupled to an auxiliary cavity. We investigate three conditions, i.e., the weak coupling regime, the intermediate coupling regime, and the strong coupling regime, by comparing the QD-photon interaction g with dipole decay rate Γ_1 and the cavity field decay rate κ in the system. The QD-photon coupling strength g and cavity-cavity coupling strength J affecting the three coupling regimes are studied, and even in weak coupling and intermediate coupling regimes, the absorption spectra can present a Mollow triplet [24] by controlling the coupling strength J. Further, under different parameter regimes, such as different cavity-cavity coupling strengths J and different pump detuning Δ_p, the absorption spectra of the QD show remarkable VRS, which indicates strong light-matter coupling in the hybrid system. The scheme may pave the way towards the realization of QD-based on-chip quantum photonic devices.

2. SYSTEM AND METHOD

As shown in Fig. 1(a), a C-QED system consisting of a QD embedded in a PhC nanocavity a with optical pump-probe technology [25] is coupled to an auxiliary cavity c with a single-mode waveguide, which is an ideal platform for the photon exchange between two optical cavities [26]. Here, we take a Fabry–Perot C-QED system as an example, and it allows generalization to other physical implementations, such as PhC nanocavity QED [10] and solid-state circuit QED systems [27]. Cavity a and cavity c are coupled with coupling strength J by exchanging energy [28], and J depends on the distance between the two cavities. The cavity-cavity coupling rate J can be efficiently tuned by changing the distance between them [29]. When coupling strength J is weak in between the two cavities, then the energy from cavity a cannot transfer easily to cavity c. Conversely, if the coupling strength J increases by decreasing the distance between the two cavities, then the energy can easily flow from the two cavities. The cavity-cavity coupling Hamiltonian [30] can be described as $H_{ac} = \hbar J(a^+c + ac^+)$. We consider the QD as a two-level system, which includes the ground state $|g\rangle$ and the single exciton state $|e\rangle$ [31] at low temperature, whose Hamiltonian is described as $H_{QD} = \hbar\omega_e\sigma^z$, with the exciton frequency ω_e, where σ^z and $\sigma^{\pm}$ are the Pauli operators. Herein, the pump field with frequency ω_p drives only the cavity mode a with a frequency ω_a. Considering a strong pump field and a weak probe field simultaneously irradiating to the QD, the Hamiltonian of the QD coupled to the two laser fields [32] is $H_{QD\text{-}F} = -\mu E_p(\sigma^+e^{-i\omega_p t} + \sigma^-e^{i\omega_p t}) - \mu E_s(\sigma^+e^{-i\omega_s t} + \sigma^-e^{i\omega_s t})$, where μ is the electric dipole moment of the exciton, ω_p and ω_s are the frequency of the two fields, and E_p (E_s) is the slowly varying envelope of the pump field (probe field).

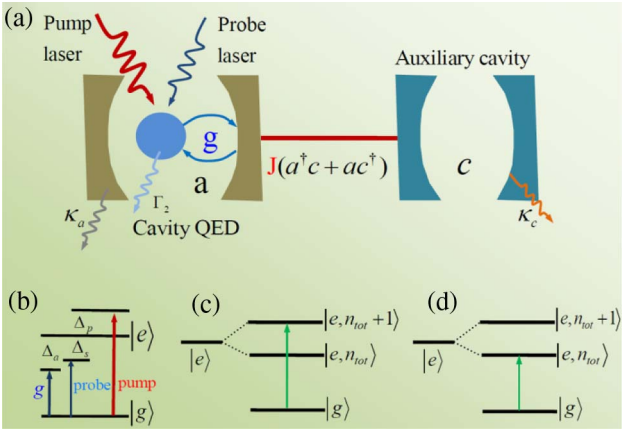

Fig. 1. (a) Schematic of the C-QED system coupled to an auxiliary cavity, and the two cavities coupled to each other via the photon-hopping interaction; (b) two energy levels of a QD coupled to a single-cavity mode and two optical fields; (c) and (d) are the energy level transitions with an entangled state $|n_{\text{tot}}\rangle$ (n_a and n_c represent the number state of the photon mode of cavity a and cavity c; $n_{\text{tot}} = n_a + n_c$ is the total photon number of the two cavities).

We use the rotating frame of the pump laser frequency ω_p and obtain the whole Hamiltonian of the system as

$$H = \hbar\Delta_p\sigma^z + \hbar\Delta_a a^+a + \hbar\Delta_c c^+c + \hbar g(\sigma^+a + \sigma^-a^+) + \hbar J(a^+c + ac^+) - \hbar\Omega_p(\sigma^+ - \sigma^-) - \mu E_s(\sigma^+e^{-i\delta t} + \sigma^-e^{i\delta t}), \tag{1}$$

where $\Delta_p = \omega_e - \omega_p$ is the exciton-pump field detuning, $\Delta_a = \omega_a - \omega_p$ is the PhC nanocavity-pump field detuning, $\Delta_c = \omega_c - \omega_p$ is the auxiliary cavity-pump field detuning, and $\delta = \omega_s - \omega_p$ is the probe-pump detuning. a^+ (c^+) and a (c) are the creation and annihilation operators for cavity a and c, respectively. g denotes the coupling strength between the exciton in the QD and the photons in the PhC nanocavity, and $\Omega_p = \mu E_p/\hbar$ is the Rabi frequency of the pump laser. According to the Heisenberg equation of motion and introducing the corresponding damping and noise terms, we obtain the quantum Langevin equations (QLEs) as follows [33]:

$$\partial_t\sigma^z = -\Gamma_1(\sigma^z + 1) - ig(\sigma^+a - \sigma^-a^+) + i\Omega_p(\sigma^+ - \sigma^-) + \frac{i\mu E_s}{\hbar}(\sigma^+e^{-i\delta t} - \sigma^-e^{i\delta t}), \tag{2}$$

$$\partial_t\sigma^- = -(i\Delta_p + \Gamma_2)\sigma^- + 2iga\sigma^z - 2i\Omega_p\sigma^z - \frac{2i\mu E_s\sigma^z e^{-i\delta t}}{\hbar} + \tau_{in}(t), \tag{3}$$

$$\partial_t a = -(i\Delta_a + \kappa_a/2)a - ig\sigma^- - iJc + a_{in}(t), \tag{4}$$

$$\partial_t c = -(i\Delta_c + \kappa_c/2)c - iJa + c_{in}(t), \tag{5}$$

where Γ_1 (Γ_2) is the exciton relaxation rate (dephasing rate), and κ_a and κ_c are the decay rate of cavity a and c, respectively. $\tau_{in}(t)$ [$a_{in}(t)$ and $c_{in}(t)$] is the δ correlated Langevin noise operator with zero mean obeying the correlation function $\langle\tau_{in}(t)\tau_{in}^+(t')\rangle \sim \delta(t-t')$ [$\langle a_{in}(t)a_{in}^+(t')\rangle \sim \delta(t-t')$, $\langle c_{in}(t)c_{in}^+(t')\rangle \sim \delta(t-t')$].

As the probe laser is weaker than the pump laser, the Heisenberg operator O can be rewritten as the sum of its steady-state mean value O_0 and a small fluctuation δO with zero mean value $\langle\delta O\rangle = 0$, i.e., $O = O_0 + \delta O$ ($O = \sigma^z, \sigma^-, a, c$)

with the standard methods of quantum optics. The steady-state values determine the steady-state population inversion ($w_0 = \sigma_0^z$) of the exciton, which obeys the equation

$$\Gamma_1(w_0+1)\{4g^2w_0^2(\Delta_c^2+\kappa_c^2/4)-2g^2w_0[2J^2(\Delta_p\Delta_c+\Gamma_2\kappa_c)+\Delta_c^2(\Gamma_2\kappa_a-2\Delta_p\Delta_a)+\kappa_c^2(\Gamma_2\kappa_a/2-\Delta_p\Delta_a)]+(\Delta_p^2+\Gamma_2^2)\Xi\}+4w_0\Gamma_2\Omega_p^2\Xi=0, \tag{6}$$

where

$$\Xi=(\Delta_a^2+\kappa_a^2/4)(\Delta_c^2+\kappa_c^2/4)+J^2(\kappa_a\kappa_c/2-2\Delta_a\Delta_c)+J^4. \tag{7}$$

Keeping only the linear terms of the fluctuation operators, we make the ansatz [32] $\langle\delta O\rangle = O_+e^{-i\delta t}+O_-e^{i\delta t}$. Solving the equation set and working to the lowest order in E_s but to all orders in E_c, we obtain the linear susceptibility as $\chi_{\text{eff}}^{(1)}(\omega_s)=\mu S_+(\omega_s)/E_s=\Sigma_1\chi^{(1)}(\omega_s)$ with $\Sigma_1=\mu^2/\hbar\Gamma_2$, and $\chi^{(1)}(\omega_s)$ is given by

$$\chi^{(1)}(\omega_s)=\frac{[\varepsilon_7\Pi_1(\Lambda_4+\varepsilon_6\Pi_2)-2iw_0\Lambda_4]\Gamma_2}{\Lambda_1\Lambda_4+\varepsilon_5\varepsilon_6\Pi_1\Pi_2}, \tag{8}$$

where $\Pi_1=2i(ga_0-\Omega_p)$, $\Pi_2=2i(ga_0^*-\Omega_p)$, $\varepsilon_1=\frac{-iJ}{i(\Delta_c-\delta)+\kappa_c/2}$, $\varepsilon_2=\frac{-iJ}{i(\Delta_c+\delta)+\kappa_c/2}$, $\varepsilon_3=\frac{-ig}{i(\Delta_c-\delta+J\varepsilon_1)+\kappa_a/2}$, $\varepsilon_4=\frac{-ig}{i(\Delta_c+\delta+J\varepsilon_2)+\kappa_a/2}$, $\varepsilon_5=\frac{i(ga_0^*-\Omega_p-g\sigma_0^*\varepsilon_3)}{\Gamma_1-i\delta}$, $\varepsilon_6=\frac{i(\Omega_p+g\sigma_0\varepsilon_4^*-ga_0)}{\Gamma_1-i\delta}$, $\varepsilon_7=\frac{i\sigma_0^*}{\Gamma_1-i\delta}$, $\varepsilon_8=\frac{i(ga_0^*-\Omega_p-g\sigma_0^*\varepsilon_4)}{\Gamma_1+i\delta}$, $\varepsilon_9=\frac{i(\Omega_p+g\sigma_0\varepsilon_3-ga_0)}{\Gamma_1+i\delta}$, $\varepsilon_{10}=\frac{i\sigma_0}{\Gamma_1+i\delta}$, $\Lambda_1=i(\Delta_p-\delta)+\Gamma_2-\Pi_1\varepsilon_5-2igw_0\varepsilon_3$, $\Lambda_2=-i(\Delta_p-\delta)+\Gamma_2-\Pi_2\varepsilon_9-2igw_0\varepsilon_3^*$, $\Lambda_3=i(\Delta_p+\delta)+\Gamma_2-\Pi_1\varepsilon_8-2igw_0\varepsilon_4$, and $\Lambda_4=-i(\Delta_p+\delta)+\Gamma_2+\Pi_2\varepsilon_6+2igw_0\varepsilon_4^*$ ($\Re^*$ indicates the conjugate of $\Re$). The imaginary and real parts of $\chi^{(1)}(\omega_s)$ indicate absorption and dispersion, respectively.

3. NUMERICAL RESULTS AND DISCUSSION

We choose the realistic coupled system of an InAs/GaAs QD embedded in a PhC nanocavity [10] in the simultaneous presence of a strong pump laser and a weak probe laser as shown in Fig. 1(a); the realistic parameters [34] of the system are $\kappa_a=\kappa_c=8$ MHz, $\Gamma_1=2\Gamma_2=5.2$ MHz. J is the coupling strength between the two cavities, which strongly depends on the distance between the two cavities [35], and the coupling strength we expect is $J/2\pi\sim$ MHz. By comparing the QD-photon interaction g with dipole decay rate Γ_1 and cavity field decay rate κ_a, we investigate three conditions, i.e., weak coupling regime ($g=2$ MHz, $g<\Gamma_1,\kappa_a$), intermediate coupling regime ($g=6$ MHz, $g\sim\Gamma_1,\kappa_a$), and strong coupling regime ($g=30$ MHz, $g>\Gamma_1,\kappa_a$), in the system.

There are two kinds of coupling in the hybrid C-QED system, i.e., exciton-photon coupling g and cavity-cavity coupling J, which will affect the dynamics of the system. Then, we should investigate the absorption properties of QD under different parameter regimes in resonant detuning $\Delta_p=0$, $\Delta_a=0$, and $\Delta_c=0$. In Fig. 2 we show how absorption spectra versus the probe detuning $\Delta_s=\omega_s-\omega_e$ change with the exciton-photon coupling g and cavity-cavity coupling J in three different cases, including the weak coupling regime ($g<\Gamma_1,\kappa_a$) in Fig. 2(a), the intermediate coupling regime ($g\sim\Gamma_1,\kappa_a$) in Fig. 2(b), and the strong coupling regime ($g>\Gamma_1,\kappa_a$) in Fig. 2(c), respectively. Obviously, when the exciton-photon coupling is $g=0$ (i.e., a pure QD system), the absorption presents a Lorentz line shape. However, when $g\neq0$, the absorption spectra experience an absorption peak to the normal splitting from a weak coupling regime to a strong coupling regime. Moreover, when we further consider the cavity-cavity coupling J, the absorption spectra display significant distinction. In the weak coupling regime [$g=2$ MHz and $J=1.0\kappa_a$ in Fig. 2(a)], although the absorption still presents a central Lorentzian peak, the full width at half-maximum is decreased and the absorption intensity is enhanced compared with a single QD in the single PhC cavity system. In the intermediate coupling regime [$g=6$ MHz and $J=1.0\kappa_a$ in Fig. 2(b)], the absorption shows a Mollow triplet, and such a Mollow triplet can be observed only in strong coupling regimes in the cavity and the emitter system [24]. In the strong coupling regime [$g=30$ MHz and $J=1.0\kappa_a$ in Fig. 2(c)], the absorption presents more remarkable Rabi splitting, and an absorption peak also arises at $\Delta_s=0$ compared with the condition of $J=0$. From the above discussion, we can draw a conclusion that the evolution of absorption depends strongly on the exciton-nanocavity coupling strength g and cavity-cavity coupling strength J.

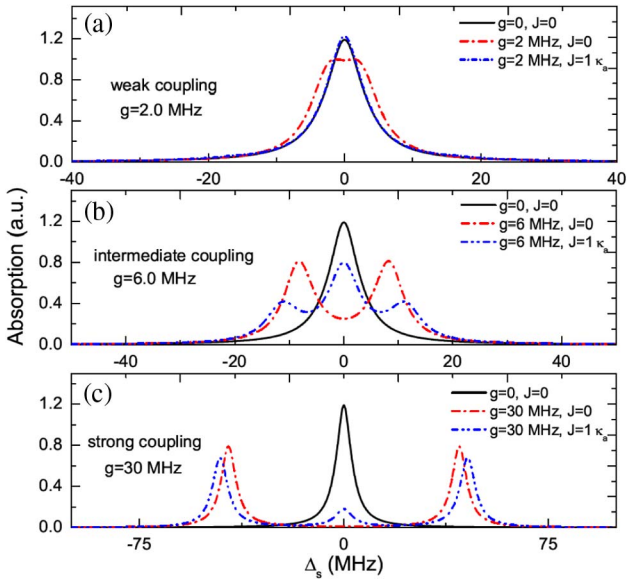

Fig. 2. (a)–(c) Probe absorption spectra of the probe field as a function of probe detuning Δ_s at $\Delta_p=0$ under three conditions, i.e., weak coupling, intermediate coupling, and strong coupling regimes. The parameters used are $\Gamma_1=5.2$ MHz, $\kappa_a=\kappa_c=8.0$ MHz, $\Omega_{pu}^2=1.0\,(\text{MHz})^2$, $\Delta_a=0$, $\Delta_c=0$.

Because the cavity-cavity coupling will affect the absorption of the QD and the absorption spectra vary significantly from the weak coupling regime to the strong coupling regime, then in the following we will investigate the parameter J in detail under different coupling regimes. We first consider the weak coupling regime ($g=2$ MHz). In the weak coupling regime, the Purcell effect [36] can either enhance or inhibit the decay rate of irreversible spontaneous emission. Figure 3 presents the probe absorption spectra as a function of probe detuning Δ_s

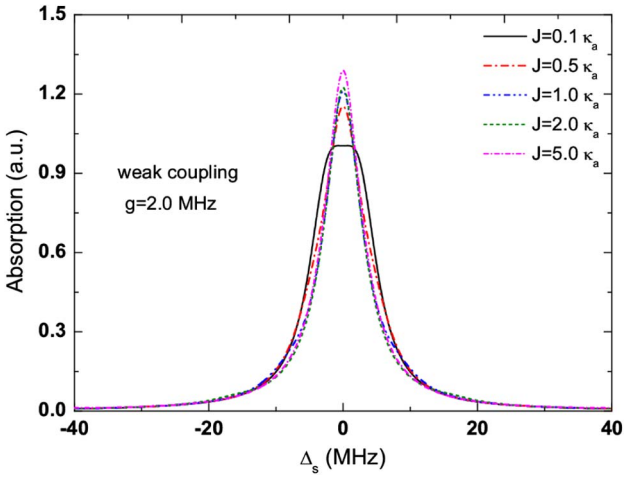

Fig. 3. Probe absorption spectra as a function of cavity-cavity coupling strength J in the weak coupling regime ($g = 2.0$ MHz). The other parameters are the same as in Fig. 2.

with several different cavity-cavity couplings J when the pump is on resonance ($\Delta_p = 0$). With the increase of the coupling strength J from $J = 0.1\kappa_a$ to $J = 5.0\kappa_a$, the probe absorption spectral intensity is enhanced and the full width at half-maximum is decreased.

Second, in the intermediate coupling regime ($g = 6$ MHz), the probe absorption spectra will change from double peaks to triple peaks under different cavity-cavity coupling J, as shown in Fig. 4. When $J = 0.1\kappa_a$, the absorption spectrum presents two peaks as normal mode splitting, and the width of splitting relies on the exciton-photon coupling strength g. With the increasing of the coupling strength J, a third peak appears in the absorption spectrum, and the middle peak is enhanced, while the two side peaks are weakened. We termed the phenomenon of the triple peaks as a quasi-Mollow triplet, which is demonstrated in a strong coupling C-QED system [24]. Therefore, the phenomenon of a quasi-Mollow triplet can arise in our system even in the intermediate coupling regime by controlling the cavity-cavity coupling. That is to say, the auxiliary cavity c plays a key role, and even in the intermediate coupling regime, a quasi-Mollow triplet can also appear in the hybrid C-QED system, which provides a scheme to investigate Mollow triplets in weak or intermediate coupling regimes.

Third, in the strong coupling regime ($g = 30$ MHz), the peak-splitting in the absorption spectra is a VRS based on C-QED, as shown in Fig. 5. Strong light-matter coupling manifested by Rabi splitting has been demonstrated in the QD-PhC cavity system [37,38]. Here, when we consider the role of the auxiliary cavity c, the VRS will vary significantly. In Fig. 5, when the cavity-cavity coupling is weak, such as $J = 1.0\kappa_a$, the absorption presents the normal Rabi splitting that is demonstrated in a QD-PhC cavity system [37,38]. This manifests itself as two distinct Lorentzian peaks and an anticrossing behavior. The phenomenon can be interpreted with a dressed-state picture. When the QD coupled to the PhC cavity, the excited state of the exciton $|e\rangle$ is dressed by an entangled state $|n_{\text{tot}}\rangle$, satisfying the total photon number of the two cavities $n_{\text{tot}} = n_a + n_c$ (n_a and n_c represent the number state of the photon mode of cavity a and cavity c). Then the original eigenstates $|e\rangle$ are modified to form two dressed states, i.e., $|e, n_{\text{tot}}\rangle$ and $|e, n_{\text{tot}} + 1\rangle$. The left sharp peak indicates the transition from $|g\rangle$ to $|e, n_{\text{tot}} + 1\rangle$, and the right sharp peak is the transition from $|g\rangle$ to $|e, n_{\text{tot}}\rangle$. With increasing the coupling strength J from $J = 1.0\kappa_a$ to $J = 5.0\kappa_a$, the splitting of the two side peaks is more remarkable, and one absorption peak will also appear in the absorption spectra at $\Delta_s = 0$. In the excitation of a strong pump field to cavity a, the steady-state entanglement state $|n_{\text{tot}}\rangle$ between cavity a and c, as a quantum channel, can be generated, which provides an indirect optical pathway to excite cavity c by means of the pump field. Therefore, the coupling strength J of the two cavities is an important factor of the quantum channel, which can influence the width of the Rabi splitting and induce one absorption at $\Delta_s = 0$.

When the pump field is detuned from the exciton transition ($\Delta_p \neq 0$), the scenario of absorption becomes completely

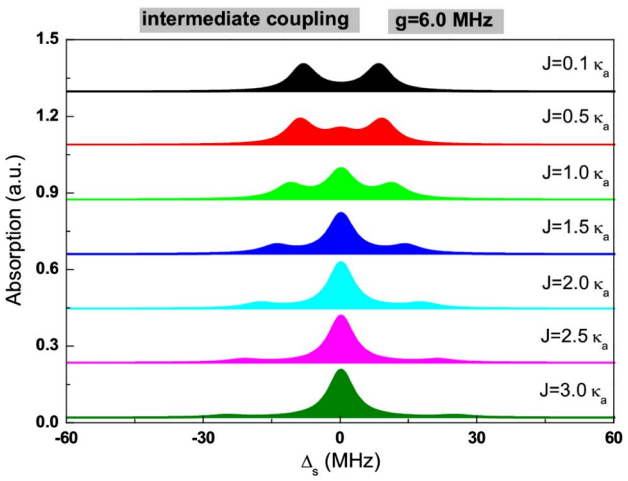

Fig. 4. Probe absorption spectra as a function of cavity-cavity coupling strength J in the intermediate coupling regime ($g = 6.0$ MHz). The other parameters are the same as in Fig. 2.

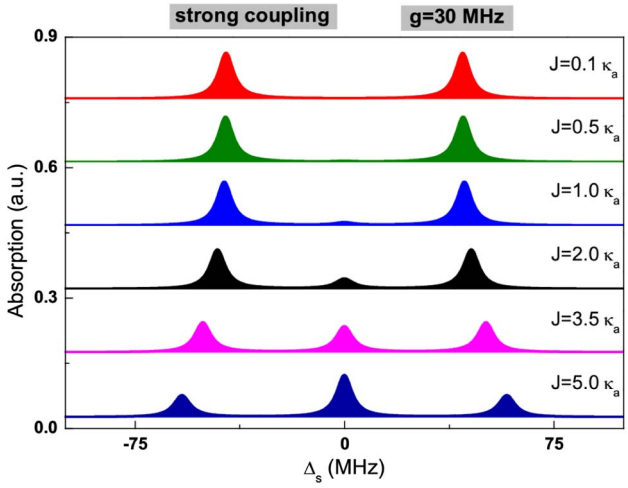

Fig. 5. Probe absorption spectra as a function of cavity-cavity coupling strength J in the strong coupling regime ($g = 30$ MHz). The other parameters are the same as in Fig. 2.

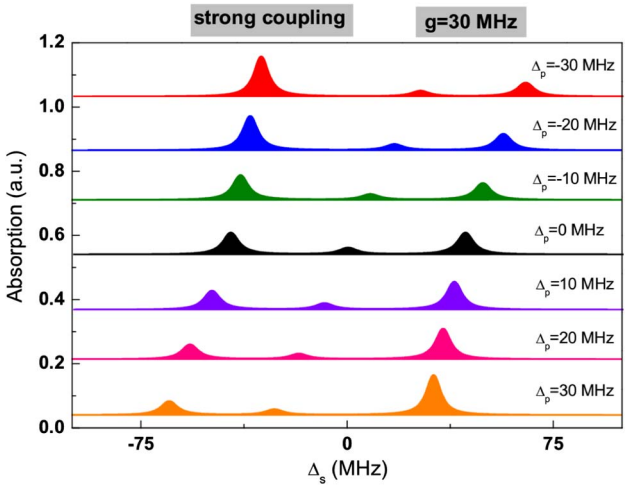

Fig. 6. Probe absorption spectra as a function of the pump frequency detuning Δ_p in the strong coupling regime ($g = 30$ MHz). $J = 2.0\kappa_a$, $\Omega_p^2 = 20\,(\mathrm{MHz})^2$, and the other parameters are the same as in Fig. 2.

different. Figure 6 shows the probe absorption spectra as a function of the pump frequency detuning Δ_p, with fixed pump intensity $\Omega_p^2 = 20\,(\mathrm{MHz})^2$. Different from the condition of the exciton-pump field detuning $\Delta_p = 0$ in Figs. 4 and 5, the probe absorption splits into a doublet where each peak has equal strength presenting symmetrical splitting. However, when $\Delta_p \neq 0$, the absorption peaks corresponding to the splitting are asymmetric, and a prominent avoided crossing phenomenon occurs in the system [23]. By increasing the detuning Δ_p, the location of the Lorentzian peaks has a frequency shift. This behavior may be ascribed to the off-resonant coupling between the QD and the PhC nanocavity. In addition, vacuum Rabi oscillation is direct evidence of the coherent energy exchange between the emitter and the cavity photon field. On the other hand, the probe absorption splits into two resonances, known as the Autler–Townes (AT) splitting, which is also observed in strongly driven QD systems [25]. In their work, the probe absorption spectra display symmetrical splitting when the pump is on resonance (i.e., $\Delta_p = 0$), and show asymmetric splitting at off-resonance (i.e., $\Delta_p \neq 0$). When we consider an auxiliary cavity, the evolution of the Rabi splitting changes significantly, and the probe absorption spectra are very different from a single QD system. This further demonstrates the role of the auxiliary cavity in the hybrid system, and the auxiliary cavity c indeed provides a quantum channel to affect the probe absorption. Obviously, the absorption spectra can be modified effectively via the off-resonant coupling between the QD and the PhC nanocavity.

4. CONCLUSION

We have designed a C-QED system consisting of a QD with optical pump-probe technology implanted in a PhC cavity that is coupled to an auxiliary cavity and investigated three kinds of coupling regimes, i.e., the weak coupling regime, intermediate coupling regime, and strong coupling regime based on the hybrid system. The probe absorption spectra show that the auxiliary cavity offers a quantum channel to influence the absorption of the probe laser. The cavity-cavity coupling plays a key role in the system, and a Mollow triplet can appear in the intermediate coupling regime rather than the strong coupling regime by adjusting the coupling strength. We also research the VRS in the absorption spectra in the strong coupling regime, which manifests in strong light-matter interactions. This study affords a platform to research QD-based C-QED systems and chip-scale nanophotonic devices.

Note added: During the submission of our paper, I became aware of a recent paper by Lichtmannecker and co-workers [39], in which they experimentally demonstrated the coexistence of weak and strong coupling with a QD in a photonic molecule. The theoretical model used in the current work is different from those described in Ref. [39].

Funding. National Natural Science Foundation of China (NSFC) (11647001, 11804004); Natural Science Foundation of Anhui Province (1708085QA11).

REFERENCES

1. H. Mabuchi and A. C. Doherty, "Cavity quantum electrodynamics: coherence in context," Science **298**, 1372–1377 (2002).
2. K. J. Vahala, "Optical microcavities," Nature **424**, 839–846 (2003).
3. C. Monroe, "Quantum information processing with atoms and photons," Nature **416**, 238–246 (2002).
4. C. Guerlin, J. Bernu, S. Deleglise, C. Sayrin, S. Gleyzes, S. Kuhr, M. Brune, J.-M. Raimond, and S. Haroche, "Progressive field-state collapse and quantum non-demolition photon counting," Nature **448**, 889–893 (2007).
5. J. L. O'Brien, A. Furusawa, and J. Vuckovic, "Photonic quantum technologies," Nat. Photonics **3**, 687–695 (2009).
6. Y.-C. Liu, Y.-F. Xiao, B.-B. Li, X.-F. Jiang, Y. Li, and Q. Gong, "Coupling of a single diamond nanocrystal to a whispering-gallery microcavity: photon transportation benefitting from Rayleigh scattering," Phys. Rev. A **84**, 011805 (2011).
7. A. Majumdar, M. Bajcsy, and J. Vuckovic, "Design and analysis of photonic crystal coupled cavity arrays for quantum simulation," Phys. Rev. A **85**, 041801 (2012).
8. J. P. Reithmaier, G. Sek, A. Loffler, C. Hofmann, S. Kuhn, S. Reitzenstein, L. V. Keldysh, V. D. Kulakovskii, T. L. Reinecke, and A. Forchel, "Strong coupling in a single quantum dot-semiconductor microcavity system," Nature **432**, 197–200 (2004).
9. E. Peter, P. Senellart, D. Martrou, A. Lemaitre, J. Hours, J. M. Gerard, and J. Bloch, "Exciton-photon strong-coupling regime for a single quantum dot embedded in a microcavity," Phys. Rev. Lett. **95**, 067401 (2005).
10. T. Yoshie, A. Scherer, J. Hendrickson, G. Khitrova, H. M. Gibbs, G. Rupper, C. Ell, O. B. Shchekin, and D. G. Deppe, "Vacuum Rabi splitting with a single quantum dot in a photonic crystal nanocavity," Nature **432**, 200–203 (2004).
11. M. Nomura, N. Kumagai, S. Iwamoto, Y. Ota, and Y. Arakawa, "Laser oscillation in a strongly coupled single quantum-dot-nanocavity system," Nat. Phys. **6**, 279–283 (2010).
12. S. Noda, M. Fujita, and T. Asano, "Spontaneous-emission control by photonic crystals and nanocavities," Nat. Photonics **1**, 449–458 (2007).
13. W.-H. Chang, W.-Y. Chen, H.-S. Chang, T.-P. Hsieh, J.-I. Chyi, and T.-M. Hsu, "Efficient single-photon sources based on low-density quantum dots in photonic-crystal nanocavities," Phys. Rev. Lett. **96**, 117401 (2006).
14. R. Johne, N. A. Gippius, G. Pavlovic, D. D. Solnyshkov, I. A. Shelykh, and G. Malpuech, "Entangled photon pairs produced by a quantum dot strongly coupled to a microcavity," Phys. Rev. Lett. **100**, 240404 (2008).

15. K. Hennessy, A. Badolato, M. Winger, D. Gerace, M. Atature, S. Gulde, S. Falt, E. L. Hu, and A. Imamoglu, "Quantum nature of a strongly coupled single quantum dot-cavity system," Nature **445**, 896–899 (2007).
16. T. Volz, A. Reinhard, M. Winger, A. Badolato, K. J. Hennessy, E. L. Hu, and A. Imamoglu, "Ultrafast all-optical switching by single photons," Nat. Photonics **6**, 605–609 (2012).
17. R. Bose, D. Sridharan, H. Kim, G. S. Solomon, and E. Waks, "Low-photon-number optical switching with a single quantum dot coupled to a photonic crystal cavity," Phys. Rev. Lett. **108**, 227402 (2012).
18. A. Reinhard, T. Volz, M. Winger, A. Badolato, K. J. Hennessy, E. L. Hu, and A. Imamoglu, "Strongly correlated photons on a chip," Nat. Photonics **6**, 93–96 (2012).
19. H. Kim, R. Bose, T. C. Shen, G. S. Solomon, and E. Waks, "A quantum logic gate between a solid-state quantum bit and a photon," Nat. Photonics **7**, 373–377 (2013).
20. A. Badolato, K. Hennessy, M. Atature, J. Dreiser, E. Hu, P. M. Petroff, and A. Imamoglu, "Deterministic coupling of single quantum dots to single nanocavity modes," Science **308**, 1158–1161 (2005).
21. D. Englund, A. Faraon, I. Fushman, N. Stoltz, P. Petroff, and J. Vuckovic, "Controlling cavity reflectivity with a single quantum dot," Nature **450**, 857–861 (2007).
22. A. Faraon, I. Fushman, D. Englund, N. Stoltz, P. Petroff, and J. Vuckovic, "Coherent generation of non-classical light on a chip via photon-induced tunnelling and blockade," Nat. Phys. **4**, 859–863 (2008).
23. Y. C. Liu, X. Luan, H. K. Li, Q. Gong, C. W. Wong, and Y. F. Xiao, "Coherent polariton dynamics in coupled highly dissipative cavities," Phys. Rev. Lett. **112**, 213602 (2014).
24. E. del Valle and F. P. Laussy, "Mollow triplet under incoherent pumping," Phys. Rev. Lett. **105**, 233601 (2010).
25. X. Xu, B. Sun, P. R. Berman, D. G. Steel, A. S. Bracker, D. Gammon, and L. J. Sham, "Coherent optical spectroscopy of a strongly driven quantum dot," Science **317**, 929–932 (2007).
26. Y.-F. Xiao, M. Li, Y.-C. Liu, Y. Li, X. Sun, and Q. Gong, "Asymmetric Fano resonance analysis in indirectly coupled microresonators," Phys. Rev. A **83**, 019902 (2011).
27. H. Toida, T. Nakajima, and S. Komiyama, "Vacuum Rabi splitting in a semiconductor circuit QED system," Phys. Rev. Lett. **110**, 066802 (2013).
28. J. Q. Liao, Q. Q. Wu, and F. Nori, "Entangling two macroscopic mechanical mirrors in a two-cavity optomechanical system," Phys. Rev. A **89**, 014302 (2014).
29. B. Peng, S. K. Ozdemir, F. Lei, F. Monifi, M. Gianfreda, G. L. Long, S. Fan, F. Nori, C. M. Bender, and L. Yang, "Parity-time-symmetric whispering-gallery microcavities," Nat. Phys. **10**, 394–398 (2014).
30. H. Jing, S. K. Ozdemir, X. Y. Lu, J. Zhang, L. Yang, and F. Nori, "PT-symmetric phonon laser," Phys. Rev. Lett. **113**, 053604 (2014).
31. A. Zrenner, E. Beham, S. Stufler, F. Findeis, M. Bichler, and G. Abstreiter, "Coherent properties of a two-level system based on a quantum-dot photodiode," Nature **418**, 612–614 (2002).
32. R. W. Boyd, *Nonlinear Optics* (Academic, 2008).
33. D. F. Walls and G. J. Milburn, *Quantum Optics* (Springer, 1994), p. 245.
34. L. M. Duan and H. J. Kimble, "Scalable photonic quantum computation through cavity-assisted interactions," Phys. Rev. Lett. **92**, 127902 (2004).
35. L. Chang, X. Jiang, S. Hua, C. Yang, J. Wen, L. Jiang, G. Li, G. Wang, and M. Xiao, "Parity-time symmetry and variable optical isolation in active-passive-coupled microresonators," Nat. Photonics **8**, 524–529 (2014).
36. E. M. Purcell, H. C. Torrey, and R. V. Pound, "Resonance absorption by nuclear magnetic moments in a solid," Phys. Rev. **69**, 37–38 (1946).
37. J. J. Li and K. D. Zhu, "A quantum optical transistor with a single quantum dot in a photonic crystal nanocavity," Nanotechnology **22**, 055202 (2011).
38. Y. C. Yu, J. F. Liu, X. L. Zhuo, G. Chen, C. J. Jin, and X. H. Wang, "Vacuum Rabi splitting in a coupled system of single quantum dot and photonic crystal cavity: effect of local and propagation Green's functions," Opt. Express **21**, 23486–23497 (2013).
39. S. Lichtmannecker, M. Kaniber, S. Echeverri-Arteaga, I. C. Andrade, J. Ruiz-Rivas, T. Reichert, M. Becker, M. Blauth, G. Reithmaier, P. L. Ardelt, M. Bichler, E. A. Gomez, H. Vinck-Posada, E. del Valle, and J. J. Finley, "Coexistence of weak and strong coupling with a quantum dot in a photonic molecule," arXiv:1806.10160v1 (2018).